JOURNAL OF COMPUTATIONAL BIOLOGY
Volume 13, Number 3, 2006

Pp. 745–766

A Stability Boundary Based Method for Finding Saddle Points on Potential Energy Surfaces

CHANDAN K. REDDY and HSIAO-DONG CHIANG

ABSTRACT

The task of finding saddle points on potential energy surfaces plays a crucial role in understanding the dynamics of a micromolecule as well as in studying the folding pathways of macromolecules like proteins. The problem of finding the saddle points on a high dimensional potential energy surface is transformed into the problem of finding decomposition points of its corresponding nonlinear dynamical system. This paper introduces a new method based on TRUST-TECH (TRansformation Under STability reTained Equilibria CHaracterization) to compute saddle points on potential energy surfaces using stability boundaries. Our method explores the dynamic and geometric characteristics of stability boundaries of a nonlinear dynamical system. A novel trajectory adjustment procedure is used to trace the stability boundary. Our method was successful in finding the saddle points on different potential energy surfaces of various dimensions. A simplified version of the algorithm has also been used to find the saddle points of symmetric systems with the help of some analytical knowledge. The main advantages and effectiveness of the method are clearly illustrated with some examples. Promising results of our method are shown on various problems with varied degrees of freedom.

Key words: potential energy surfaces, saddle points, stability boundary, minimum gradient point, computational chemistry.

I. INTRODUCTION

RECENTLY, THERE HAS BEEN A LOT OF INTEREST across various disciplines to understand a wide variety of problems related to bioinformatics. One of the most challenging problems in the field of bioinformatics is de novo protein structure prediction where the structure of a protein is estimated from some complex energy functions. Scientists have related the native structure of a protein structurally to the global minimum of the potential energy surface of its energy function (Dill *et al.*, 1997). If the global minimum could be found reliably from the primary amino acid sequence, it would provide us with new insights into the nature of protein folding. However, understanding the process of protein folding involves more than just predicting the folded structures of foldable sequences. The folding pathways in which the proteins attain their native structure can deliver some important information about the properties of the protein structure (Merlo *et al.*, 2005).

School of Electrical and Computer Engineering, Cornell University, Ithaca, NY 14850.

Proteins usually have multiple stable macrostates (Erman *et al.*, 1997). The conformations associated with one macrostate correspond to a certain biological function. Understanding the transition between these macrostates is important to comprehend the interplay between that protein with its environment, and to understand the kinetics of the folding process, we need the structure of the transition state. Since, it is difficult to characterize these structures by manual experiments, simulations are an ideal tool for the characterization of the transition structures. Recently, biophysicists started exploring the computational methods that can be used to analyze conformational changes and identify possible reaction pathways (Bokinsky *et al.*, 2003). In particular, the analysis of complex transitions in macromolecules has been widely studied (Henkelman *et al.*, 2000a).

From a computational viewpoint, transition state conformations are saddle points. *Saddle points* are the points on a potential energy surface where the gradient is zero and where the Hessian of the potential energy function has only one negative eigenvalue (Heidrich *et al.*, 1991). Intuitively, this means that a saddle point is a maximum along one direction but a minimum along all other orthogonal directions. Figure 1 shows a saddle point (x_d) located between two local minima (x_s^1 and x_s^2) and two local maxima (x_m^1 and x_m^2). As shown in the figure, the saddle point is a maximum along the direction of the vector joining the two local minima and a minimum along its orthogonal direction (or the direction of the vector joining the two local maxima). The direction in which the saddle point is the maximum is usually unknown in most of the practical problems and is the direction of interest. This makes the problem of finding the saddle points more challenging than the problem of finding local minima on a potential energy surface. In terms of transition states, saddle points are local maxima with respect to the reaction coordinates for folding and local minima with respect to all other coordinates. The search for the optimal transition state becomes a search for the saddle points at the edge of the potential energy basin corresponding to the initial state. Hence, finding the saddle points on potential energy surfaces is a challenging problem and will give new insight into the folding mechanism of proteins.

The primary focus of this paper is to find the saddle points on different potential energy surfaces with varied degrees of freedom using TRUST-TECH based strategies (Chiang and Chu, 1996; Lee and Chiang, 2004). The saddle point to be found is between two known neighborhood local minima. Section II briefly describes some related methods that were developed for finding saddle points. Section III gives the necessary theoretical background of our approach and describes the problem formulation. Section IV explains the various steps involved in our approach. The implementation details along with the pseudocode of different procedures are provided in Section V. Results of our method on different systems are clearly illustrated in Section VI with some relevant discussions. Finally, conclusions and future plans of our research are discussed in Section VII.

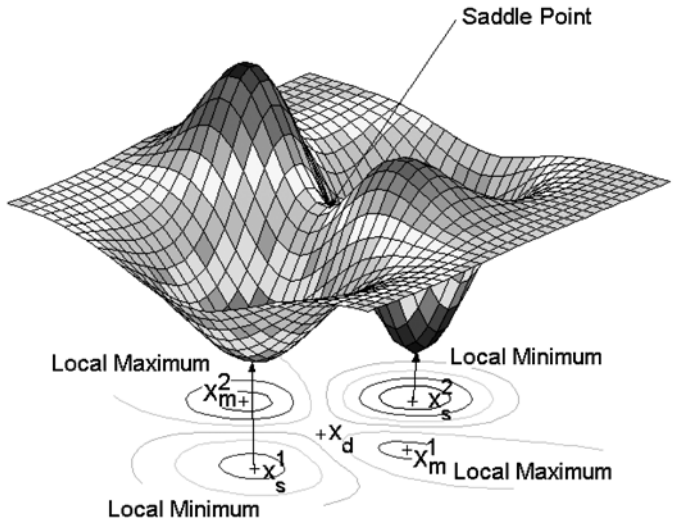

FIG. 1. The surface and contour plots of a two-dimensional energy function. A saddle point (x_d) is located between two local minima (x_s^1 and x_s^2). Points x_m^1 and x_m^2 are two local minima located in the orthogonal direction.

II. RELEVANT BACKGROUND

The task of finding saddle points has been a topic of active research in the field of computational chemistry for almost two decades. Recently, there has also been some interest in finding the saddle points of the Lennard–Jones clusters since it will give some idea about the dynamics of the system (Doye and Wales, 2002). The properties of higher-index saddle points have been invoked in recent theories of the dynamics of supercooled liquids. Since the saddle points are related to the eigenvalues of the Hessian matrix, several methods have been proposed in the literature that are based on the idea of digitalization of the Hessian matrix (Khait *et al.*, 1995; Baker, 1986; Helgaker, 1991). Some improved methods dealing with the updates of Hessian matrix have also been proposed (Quapp *et al.*, 1998). Even though these methods appear to find saddle points accurately, they work mainly for low dimensional systems. These methods are not practical for higher dimensional problems because the computational cost increases tremendously as the number of dimensions increases.

However, some methods that work without the necessity for computing the second derivatives have been developed. Because of the scalability issues, much more importance is given to the algorithms that use only the first derivatives to compute the saddle points. A detailed description of the methods that work based only on first derivatives along with their advantages and disadvantages is given in a recent review paper (Henkelman *et al.*, 2000a). The various methods that are used to find saddle points are the drag method (Henkelman *et al.*, 2000a), dimer method (Henkelman *et al.*, 1999), self-penalty walk (Czerminski and Elber, 1990), activation relaxation technique (Barkema and Mousseau, 1996), ridge method (Ionova and Carter, 1993), conjugate peak refinement (Fischer and Karplus, 1992), DHS method (Dewar *et al.*, 1984), nudged elastic band (Jonsson *et al.*, 1998; Henkelman *et al.*, 2000b), and step and slide (Miron and Fichthorn, 2001). Continuation methods for finding the saddle points are described by Lastras (1998). Almost all these methods except the dimer method are used to identify the saddle point between two given neighboring local minima. Though the dimer method successfully finds the saddle points in those cases where only one minimum is given, it does not have a good control over which saddle point it intends to find.

All these methods start searching for saddle points from the local minimum itself, and hence they need to compute the first derivative. However, our approach doesn't require the gradient information starting from the local minima. It will find the stability boundary in a given direction and then trace the stability boundary till the saddle point is reached (Reddy and Chiang, 2005). This tracing of the stability boundary is more efficient than looking for saddle points in the entire search space. This paper presents a completely novel *stability boundary* based approach to compute the saddle point between two given local minima. Our method is based on some of the fundamental results on stability regions of nonlinear dynamical systems (Chiang *et al.*, 1988; Chiang and Fekih-Ahmed, 1996; Lee and Chiang, 2004).

III. PROBLEM FORMULATION AND TRANSFORMATIONS

This section introduces some of the terminology needed to understand our approach. Most importantly, this section deals with the transformation of the potential energy function into a nonlinear dynamical system. It also gives the correspondence between all the saddle points of an n-dimensional potential energy surface and that of its nonlinear dynamical system.

A. Mathematical preliminaries

Before presenting the details of our method, we review some fundamental concepts of nonlinear dynamical systems. Let us consider an unconstrained search problem on an energy surface defined by the objective function

$$f(x) \tag{1}$$

where $f(x)$ is assumed to be in $C^2(\Re^n, \Re)$.

Definition 1. *Point $\bar{x}$ is said to be a* critical point *of (1) if it satisfies the following condition.*

$$\nabla f(\bar{x}) = 0 \tag{2}$$

A critical point is said to be nondegenerate *if at the critical point $\bar{x} \in \Re^n$, $d^T \nabla^2_{xx} f(\bar{x}) d \neq 0 \quad (\forall d \neq 0)$.*

We construct the following *negative gradient system* in order to locate critical points of the objective function (1):

$$\frac{dx}{dt} = -\nabla f(x) \tag{3}$$

where the state vector x belongs to the Euclidean space $\Re^n$ and the vector field $f : \Re^n \to \Re^n$ satisfies the sufficient condition for the existence and uniqueness of the solutions. The solution curve of Equation (3) starting from x at time $t = 0$ is called a *trajectory* and it is denoted by $\Phi(x, \cdot) : \Re \to \Re^n$. A state vector x is called an *equilibrium point* of Equation (3) if $f(x) = 0$.

Definition 2. *An equilibrium point is said to be* hyperbolic *if the Jacobian of f at point x has no eigenvalues with zero real part. A hyperbolic equilibrium point is called a (asymptotically)* stable equilibrium point (SEP) *if all the eigenvalues of its corresponding Jacobian have negative real part. Conversely, it is an* unstable equilibrium point *if some eigenvalues have a positive real part.*

An equilibrium point is called a *type-k equilibrium point* if its corresponding Jacobian has exact k eigenvalues with positive real part. When $k = 0$, the equilibrium point is (asymptotically) stable and it is called a *sink* (or *attractor*). If $k = n$, then the equilibrium point is called a *source* (or *repeller*).

A dynamical system is completely *stable* if every trajectory of the system leads to one of its stable equilibrium points. The *stable* ($W^s(\tilde{x})$) and *unstable* ($W^u(\tilde{x})$) manifolds of an equilibrium point, say $\tilde{x}$, is defined as

$$W^s(\tilde{x}) = \left\{ x \in \Re^n \ : \ \lim_{t \to \infty} \Phi(x, t) = \tilde{x} \right\}, \tag{4}$$

$$W^u(\tilde{x}) = \left\{ x \in \Re^n \ : \ \lim_{t \to -\infty} \Phi(x, t) = \tilde{x} \right\}. \tag{5}$$

The stable and unstable manifolds of an equilibrium point are said to satisfy the *transversality* condition if either they do not intersect at all, or at every intersection point x_0 between these two manifolds, the tangent spaces of $W^s(x_0)$ and $W^u(x_0)$ span $\Re^n$. This is shown in Equation (6)

$$T(W^s(x_0)) \oplus T(W^u(x_0)) = \Re^n \tag{6}$$

Definition 3. *The* stability region *(also called* region of attraction*) of a stable equilibrium point x_s of a dynamical system (3) is denoted by $A(X_s)$ and is*

$$A(x_s) = \left\{ x \in \Re^n \ : \ \lim_{t \to \infty} \Phi(x, t) = x_s \right\}. \tag{7}$$

The boundary of stability region is called the *stability boundary* of x_s and will be denoted by $\partial A(x_s)$. It has been shown that the stability region is an open, invariant, and connected set (Chiang *et al.*, 1988). From the topological viewpoint, the stability boundary is an $(n-1)$ dimensional closed and invariant set. A new concept related to the stability regions, namely, the *quasi-stability region* (or *practical stability region*), was developed by Chiang and Fekih-Ahmed (1996).

Definition 4. *The* practical stability region *of a stable equilibrium point x_s of a nonlinear dynamical system (3), denoted by $A_p(x_s)$ is*

$$A_p(x_s) = int\ \overline{A(x_s)} \tag{8}$$

where $\bar{A}$ denotes the closure of A and int $\bar{A}$ denotes the interior of $\bar{A}$. Set int $\overline{A(x_s)}$ is an open set. The boundary of practical stability region is called the practical stability boundary *of x_s and will be denoted by $\partial A_p(x_s)$.*

It has been shown that the practical stability boundary $\partial A_p(x_s)$ is equal to $\partial \bar{A}(x_s)$. The practical stability boundary is a subset of its stability boundary. It eliminates the complex portion of the stability boundary which has no "contact" with the complement of the closure of the stability region. A complete characterization of the practical stability boundary for a large class of nonlinear dynamical systems can be found in Chiang *et al.* (1988).

Definition 5. *A type-1 equilibrium point x_d $(k = 1)$ on the practical stability boundary of a stable equilibrium point x_s is called a* decomposition point.

In this paper, the task of finding saddle points is transformed into the task of finding the decomposition points on the stability boundary between two stable equilibrium points (i.e., the two local minima). The advantage of our approach is that this transformation into the corresponding dynamical system will yield more knowledge about the various dynamic and geometric characteristics of the original surface and leads to the development of a powerful method for finding saddle points.

B. Theoretical background

To comprehend the transformation, we need to define the *energy function*. A smooth function $V(\cdot) : \Re^n \to \Re^n$ satisfying $\dot{V}(\Phi(x,t)) < 0$, $\forall\, x \notin$ {set of equilibrium points (E)} and t $\in \Re^+$ is called the *energy function*.

Theorem 3.1 (Chiang and Chu, 1996). *Function $f(x)$ is a Lyapunov function for the negative quasi-gradient system (3).*

Proof. See Appendix C. ■

The stability region of a stable equilibrium point can be completely characterized for a fairly large class of nonlinear systems. Consider the gradient system described by (3) satisfying the following assumptions:

(A1) The critical elements on the stability boundary are hyperbolic and finite in number.
(A2) The stable and unstable manifolds of the critical elements on the stability boundary satisfy the transversality condition.
(A3) Every trajectory on the stability boundary approaches one of the critical elements as $t \to \infty$.

We present the conditions for an equilibrium point to be on the $\partial A(x_s)$. This is a key step in the complete characterization of $\partial A(x_s)$.

Theorem 3.2 (Chiang *et al.*, 1988). *Let $A(x_s)$ be the stability region of nonlinear dynamical system (3). Let $\sigma \neq x_s$ be a hyperbolic critical element of system (3). If assumptions (A1)–(A3) are satisfied, then*

1. $\sigma \in \partial A$ if and only if $W^u(\sigma) \cap A(x_s) \neq \emptyset$.
2. $\sigma \in \partial A$ if and only if $W^s(\sigma) \subset \partial A(x_s)$.

Theorem 3.3 (Chiang and Fekih-Ahmed, 1996). Characterization of stability boundary. *Consider a nonlinear dynamical system described by (3) which satisfy assumptions (A1)–(A3). Let σ_i, $i = 1, 2, \ldots$ be the equilibrium points on the stability boundary $\partial A(x_s)$ of a stable equilibrium point, say x_s. Then*

$$\partial A(x_s) = \bigcup_{\sigma_i \in \partial A} W^s(\sigma_i). \tag{9}$$

Theorem 3.3 completely characterizes the stability boundary for nonlinear dynamical systems satisfying assumptions (A1)–(A3) by asserting that the stability boundary is the union of the stable manifolds of all

critical elements on the stability boundary. This theorem gives an explicit description of the geometrical and dynamical structure of the stability boundary. This theorem can be extended to the characterization of the practical stability boundary in terms of the stable manifold of the decomposition point.

Theorem 3.4 (Chiang and Fekih-Ahmed, 1996). Characterization of practical stability boundary. *Consider a nonlinear dynamical system described by (3) which satisfy assumptions (A1)–(A3). Let* σ_i, $i = 1, 2, \ldots$ *be the decomposition points on the practical stability boundary* $\partial A_p(x_s)$ *of a stable equilibrium point, say* x_s. *Then*

$$\partial A_p(x_s) = \bigcup_{\sigma_i \in \partial A_p} \overline{W^s(\sigma_i)}. \tag{10}$$

Theorem 3.4 asserts that the practical stability boundary is contained in the union of the closure of the stable manifolds of all the decomposition points on the practical stability boundary. Hence, if the decomposition points can be identified, then an explicit characterization of the practical stability boundary can be established using (10).

Theorem 3.5 (Lastras, 1998). Unstable manifold of type-1 equilibrium point. *Let* x_s^1 *be a stable equilibrium point of the gradient system (3) and* x_d *be a type-1 equilibrium point on the practical stability boundary* $\partial A_p(x_s)$. *Assume that there exist* ϵ *and* δ *such that* $\|\nabla f(x)\| > \epsilon$ *unless* $x \in B_\delta(\hat{x}), \hat{x} \in \{x : \nabla f(x) = 0\}$. *If assumptions (A1)–(A3) are satisfied, then there exists another stable equilibrium point* x_s^2 *to which the one dimensional unstable manifold of* x_d *converges. Conversely, if* $\overline{A_p(x_s^1)} \bigcap \overline{A_p(x_s^2)} \neq \emptyset$, *then there exists a decomposition point* x_d *on* $\partial A_p(x_s^1)$.

Theorem 3.5 is imperative to understand some of the underlying concepts behind the development of our method. It associates the notion of stable equilibrium points, practical stability regions ($A_p(x_s)$), practical stability boundaries ($\partial A_p(x_s)$), and type-1 equilibrium points. As shown in Fig. 2, The unstable manifold

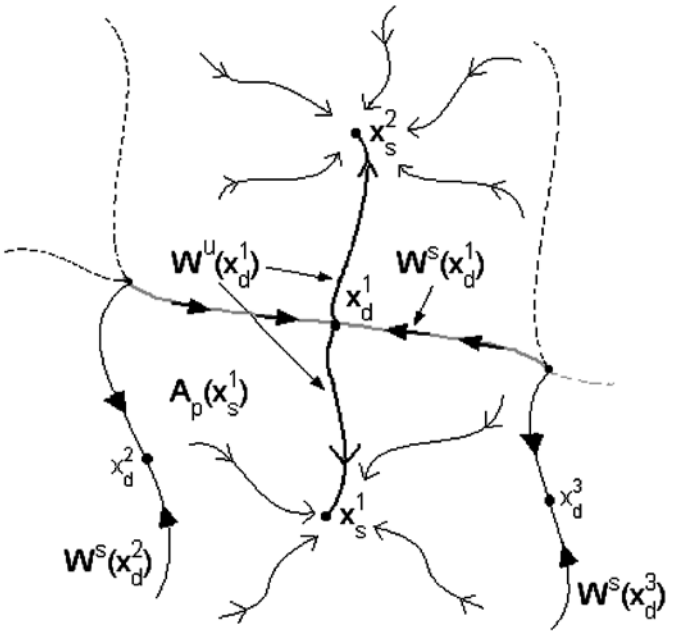

FIG. 2. Phase potrait of the gradient system corresponding to Fig. 1. The solid lines represent the basin boundary which shows that $\partial A_p(x_s^1) = \cup_{i=1}^3 \overline{W^s(x_d^i)}$. The local minima x_s^1 and x_s^2 correspond to the stable equilibrium points of the gradient system. The saddle point (x_d^1) corresponds to the decomposition point of the gradient system.

(W^u) of the decomposition point x_d^1 converges to the two stable equilibrium points x_s^1 and x_s^2. Also, it should be noted that x_d^1 is present on the stability boundary of x_s^1 and x_s^2.

We also need to show that under the transformation from (1) to (3), the properties of the critical points remain unchanged. Theorem 3.6 illustrates the correspondence of the critical points of the original system. In this paper, we are particularly interested in the properties of the saddle points and their one-to-one corrspondence to decomposition points.

Theorem 3.6 (Chiang and Chu, 1996). Critical points and their correspondence. *An equilibrium point of (3) is hyperbolic if, and only if, the corresponding critical point f is nondegenerate. Moreover, if $\bar{x}$ is a hyperbolic equilibrium point of (3), then*

1. *$\bar{x}$ is a stable equilibrium point of (3) if and only if $\bar{x}$ is an isolated local minimum for (1),*
2. *$\bar{x}$ is a source of (3) if and only if $\bar{x}$ is an isolated local maximum for (1), and*
3. *$\bar{x}$ is a decomposition point of (3) if and only if $\bar{x}$ is a saddle point for (1).*

Proof. See Appendix C. ■

IV. A STABILITY BOUNDARY BASED METHOD

Our TRUST-TECH based method uses the theoretical concepts of dynamical systems presented in the previous section. The method described in this section finds the decomposition point when the two neighborhood local minima are given. Our method is illustrated on a two-dimensional LEPS potential energy surface (Polanyi and Wong, 1969). The equations corresponding to the LEPS potential are given in the appendix. The two local minima are A and B, and the decomposition point is DP.

Given: Two neighborhood local minima (A,B)
Goal: To obtain the corresponding decomposition point (DP)

Step 1: *Initializing the search direction:* Since the location of the neighborhood local minima is already given, the initial search direction becomes explicit. The vector that joins the two given local minima (A and B) is chosen to be the initial search direction.

Step 2: *Locating the exit point (X_{ex}) (see Fig. 3):* Along the direction AB, starting from A, the function value is evaluated at different step intervals. Since the vector is between two neighborhood local minima, the function value will monotonically increase and decrease till it reaches the other local minimum (B). The point where the energy value attains its peak is called the *exit point*.

Step 3: *Moving along the stability boundary to locate the minimum gradient point:* We used a novel *trajectory adjustment procedure* to move along the practical stability boundary (see Fig. 4). Once the exit point is identified, the consecutive points on the stability boundary can be identified by this trajectory-adjustment procedure. The exit point (X_{ex}) is integrated for a predefined number of times. Let m_1' be the new point obtained after integration. The function value between m_1' and the local minimum is evaluated and the peak value is obtained. Let the new boundary point along the vector $m_1'B$ starting from the point m_1' and where the value attains the peak be m_2. This process is repeated and several points on the stability bondary are obtained. During this traversal, the value of the gradient along the boundary is noted, and the process of moving along the boundary is terminated when the minimum gradient point (MGP) is obtained. In summary, the trajectory of integration is being modified so that it moves towards the MGP and will not converge to one of the local minima. This is an intelligent TRUST-TECH based scheme for following the stability boundary which is the *heart* of the proposed method. This step is named as the trajectory-adjustment procedure.

Step 4: *Locating the decomposition point (DP):* The minimum gradient point (m_n) obtained from the previous step will be present in the neighborhood of the decomposition point. A local minimizer to solve the system of nonlinear equations is applied with m_n as initial guess, and this will yield the decomposition point. A detailed survey about different local minimizations applied to a wide variety of areas is given by Schlick (2002).

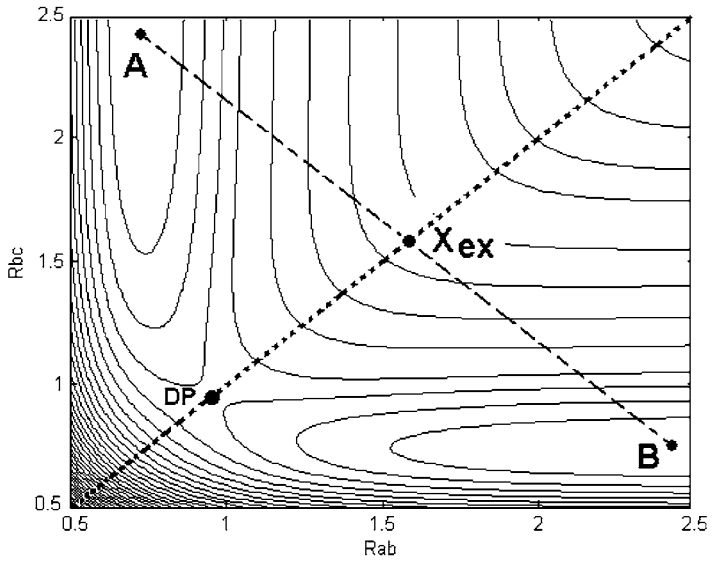

FIG. 3. Contour plot of a 2-D LEPS potential (described in Appendix A). Each line represents the values of a constant potential. Points A and B are the two local minima. Point DP is the decomposition point to be computed. The search direction is the direction of the vector joining AB. The exit point (X_{ex}) is obtained by finding the peak of the function value along this vector. The dotted line indicates the stability boundary. The dashed line indicates the search direction.

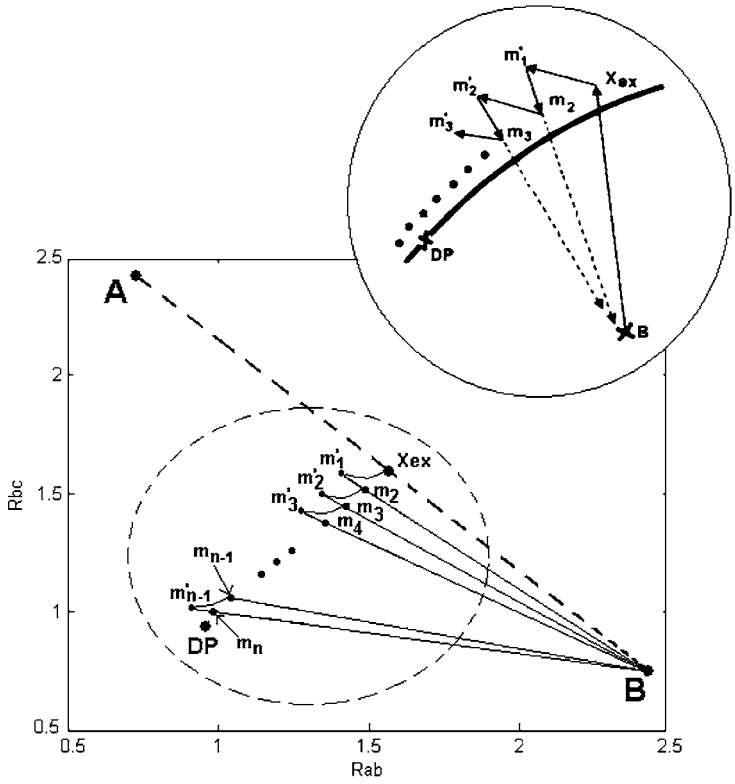

FIG. 4. Illustration of step 3 of our algorithm. X_{ex} is the exit point between A and B. X_{ex} is integrated until m'_1 is reached and traced back along the vector m'_1B to get m_2, and so on. Points m_2, $m_3, \ldots,$ are the m_n points on the stability boundary. The nth point is the minimum gradient point where the magnitude of the gradient (G_M) is the minimum. DP is the decomposition point.

Remarks:

- The step size to be chosen during the step 2 of our algorithm is very critical for faster computation and accuracy of the exit point.
- The number of integrations to be performed from a point on the stability boundary (m_k) till the new point (m'_k) is reached is problem specific and it depends on the characteristics of the stability region near the boundary.
- The minimum gradient point is usually in the neighborhood of the decomposition point. Newton's method appears to be a good choice for a local solver that can be used to obtain the decomposition point.

V. IMPLEMENTATION ISSUES

For our illustration, let's consider an N dimensional function F with variables X_i, where $i = 1 \ldots N$. From the algorithmic viewpoint, our method consists of three stages: (i) finding exit point, (ii) following stability boundary, and (iii) local minimization. Let A and B be the given local minima. The psuedocode for finding the decomposition point is as follows:

```
point procedure locate_DP(A, B)
Initialize stepsize = 10  // initial evaluation step size
EP ← find_ExitPt(A, B, stepsize)  // Exit point
MGP ← Boundary_Following(EP)  // Trace the boundary
DP ← local_minimizer(MGP)
return DP
```

```
point procedure find_ExitPt(A, B, steps)
Initialize eps // accuracy
interval = (B − A)/steps
cur = eval(A)
tmp = A + interval
if eval(tmp) < cur then
   B = 2 ∗ A − B
end if
for i = 1 to steps do
   tmp = A + i ∗ interval
   prev = cur
   cur = eval(tmp)
   if prev > cur then
      newPt = A + (i − 2) ∗ interval
      BdPt = GoldenSectionSearch(tmp, newPt, eps)
      return BdPt
   end if
end for
return NULL
```

The procedure *find_ExitPt* will find the point on the stability boundary between two given points A and B starting from A (*step 2* of our algorithm). If the function value is monotonically decreasing from the first step, then it indicates that there will not be any boundary in that direction, and the search is changed to a new direction. The new direction can be obtained by making $B = 2A - B$. Finding the exit point can be done more efficiently by first evaluating the function at comparatively large step intervals (see Fig. 5). The function evaluation is started from a_1, a_2 and so on. Once a_6 is reached, the energy value

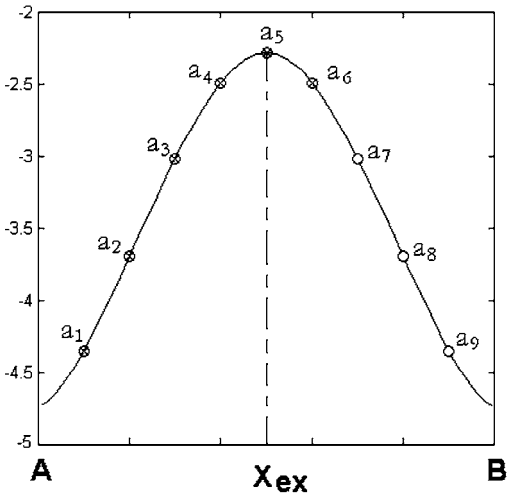

FIG. 5. The plot of the function value along the vector AB. The curve monotonically increases starting from A and then decreases until it reaches B. Point X_{ex} is the exit point where the function attains its peak value. Points $a_1, a_2, \ldots, a_9$ are the interval points. The marked circles indicate that the function has been evaluated at these points. The empty circles indicate the points where the function is yet to be evaluated.

starts to diminish indicating that the peak value has been reached. The golden section search algorithm (see appendix) is used to efficiently find the exit point within a small interval range where the peak value is present. The golden section search is applied to obtain the exit point X_{ex} within the intervals a_4 and a_6. In fact, golden section search could have been used from the two given local minima. We prefer to evaluate the function value at certain intervals because using this method the stability boundary can be identified without knowing the other local minima as well.

Figure 6 shows the other two possibilities of having the interval points. It should be noted that the golden section search procedure should not be invoked with two consecutive intervals between which the value starts to diminish. It should be applied to two intervals a_4 and a_6. The two possibilities are that a_5 can be present either to the left of the peak or to the right of the peak. From Fig. 6b, we can see that the value at a_5 is greater than a_4 and less than a_6 but still the peak is not present between a_5 and a_6. This is the reason why the golden section search method should have a_4 and a_6 as its arguments.

In an ideal case, integration from the exit point will lead to the decomposition point. However, due to the numerical approximations made, the integration at the exit point will eventually converge to its corresponding local minimum. Hence, we need to adjust the path of integration so that it can effectively trace the boundary.

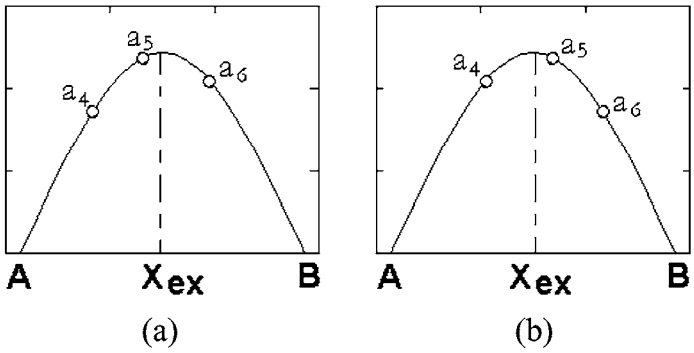

FIG. 6. The interval point a_5 can be present either to the left or to the right of the peak. When a_6 is reached, the golden section search method is invoked with a_6 and a_4 as the interval.

point **procedure** *Boundary_Following*(*ExPt*)
1: Initialize *dt* // Integral step size
2: Initialize *intsteps* // No. of integration steps
3: Initialize *smallstep* //small step size
4: *reduce_flag* = *OFF* // To check if gradient reduced
5: *BdPt* = *ExPt*
6: *GM_next* = *GM*(*BdPt*)
7: **while** (1) **do**
8: *NewPt* = *integrate*(*BdPt*, *intsteps*, *dt*)
9: *prevPt* = *BdPt*
10: *BdPt* = *find_ExitPt*(*NewPt*, *A*, *smallstep*)
11: *GM_prev* = *GM_next*
12: *GM_next* = *GM*(*BdPt*)
13: **if** *GM_next* < *GM_prev* **then**
14: *reduce_flag* = *ON*
15: **end if**
16: **if** *GM_next* > *GM_prev* & *reduce_flag* = *ON* **then**
17: *MGPt* = *prevPt*
18: **end if**
19: **return** *MGPt*
20: **end while**

The procedure *Boundary_Following* takes in the exit point as the argument and returns the computed MGP obtained by tracing the stability boundary starting from the exit point (*step 3* of our algorithm). The point on the stability boundary is integrated a predefined number of times. From the exit point, it is integrated using the equation shown below.

$$X_{(i+1)} = X_{(i)} - \left(\frac{\partial F}{\partial X_{(i)}}\right) \; . \; \Delta t \tag{11}$$

The procedure *integrate* computes a point (*newPt*) by integrating a certain number of integral steps (*intstep*) with a predefined integration step size (Δt) from the boundary point (*bdPt*). Once again a new boundary point is obtained from $newPt$ and the local minimum in the other stability region using the procedure *find_ExitPt* and this process is repeated. Another important issue to be dealt is when should we stop this process. For this, we need to compute the magnitude of the gradient at all points obtained on the stability boundary. The magnitude of the gradient (G_M) is calculated using Equation (12).

$$G_M = \sqrt{\sum_{i=1}^{N} \left(\frac{\partial F}{\partial X_i}\right)^2} \tag{12}$$

where Δt is the integral step size. The G_M value can either start increasing and then decrease or it might start decreasing from the exit point. The *reduce_flag* indicates that the G_M value started to decrease. The two variables *GM_next* and *GM_prev* are sed to store the values of the current and previous G_M values, respectively. The *MGP* is obtained when *GM_next* > *GM_prev* and *reduce_flag* = *ON*.

VI. RESULTS AND DISCUSSION

A. Test Case 1: Two-dimensional potential energy surfaces

Muller–Brown surface: The Muller–Brown surface forms a standard two-dimensional example of a potential energy function in theoretical chemistry (Muller and Brown, 1979). This surface was designed for testing the algorithms that find saddle points. Equation (13) gives the Muller–Brown energy function.

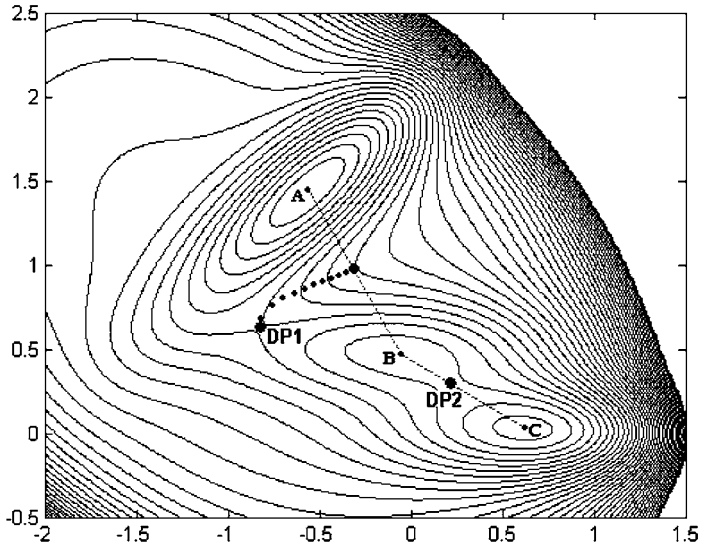

FIG. 7. Two dimensional contour plot of the potential energy surface corresponding to the Muller–Brown function described by Equation (13). Points *A*, *B*, *C* are stable equilibrium points and *DP*1, *DP*2 are two decomposition points. The dashed lines indicate the initial search direction. The dots indicate the results of the trajectory adjustment procedure. These points are the points on the stability boundary that reach the MGP.

Figure 7 represents the two-dimensional contour plot of the potential energy surface of the Muller–Brown function.

$$C(x, y) = \sum_{i=1}^{4} A_i \ \exp\left[a_i(x - x_i^o)^2 + b_i(x - x_i^o)(y - y_i^o) + c_i(y - y_i^o)^2\right] \tag{13}$$

where

$$A = (-200.0, -100.0, -170.0, -15.0) \quad a = (-1.0, -1.0, -6.5, -0.7)$$

$$x^o = (1.0, 0.0, -0.5, -1.0) \quad b = (0.0, 0.0, 11.0, 0.6)$$

$$y^o = (0.0, 0.5, 1.5, 1.0) \quad c = (-10.0, -10.0, -6.5, 0.7)$$

As shown in Fig. 7, there are three stable equilibrium points (A,B,C) and two decomposition points (DP1,DP2) on the muller-brown potential energy surface. Decomposition point 1 is present between A and B and is more challenging to find, compared to decomposition point 2 which is present between B and C. Table 1 shows the exact locations and energy values of the local minima and the decomposition points.

TABLE 1. STABLE EQUILIBRIUM POINTS AND DECOMPOSITION POINTS FOR THE MULLER–BROWN SURFACE DESCRIBED IN EQUATION (13)

Equilibrium points	*Location*	*Energy value* $c(\cdot)$
SEP A	(−0.558, 1.442)	−146.7
DP 1	(−0.822, 0.624)	−40.67
SEP B	(−0.05, 0.467)	−80.77
DP 2	(0.212, 0.293)	−72.25
SEP C	(0.623, 0.028)	−108.7

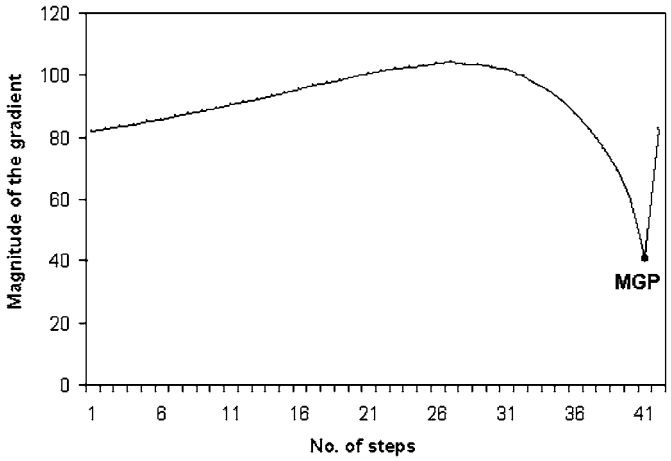

FIG. 8. The gradient curve corresponding to the various points obtained from the trajectory adjustment procedure. The graph shows that the magnitude of the gradient slowly increases in the initial phases and then starts to reduce. The highlighted point corresponds to the gradient at the MGP.

We construct the dynamical system corresponding to (13) as follows:

$$\begin{bmatrix} \dot{x}(t) \\ \dot{y}(t) \end{bmatrix} = - \begin{bmatrix} \dfrac{\partial C}{\partial x} \\ \dfrac{\partial C}{\partial y} \end{bmatrix}, \tag{14}$$

$$\frac{\partial C}{\partial x} = \sum_{i=1}^{4} A_i \ . \ P \ . \ [2a_i(x - x_i^o) + b_i(y - y_i^o)],$$

$$\frac{\partial C}{\partial y} = \sum_{i=1}^{4} A_i \ . \ P \ . \ [b_i(x - x_i^o) + 2c_i(y - y_i^o)],$$

where

$$P = \exp[a_i(x - x_i^o)^2 + b_i(x - x_i^o)(y - y_i^o) + c_i(y - y_i^o)^2].$$

The exit point obtained between the local minima A and B is (−0.313, 0.971). Figure 7 shows the results of our algorithm on a Muller–Brown surface. The dashed lines indicate the initial search vector which is used to compute the exit point. The dots indicate the points along the stability boundary obtained during the trajectory adjustment procedure These dots move from the exit point towards the MGP. The gradient curve corresponding to the points along this stability boundary is shown in Fig. 8. From the MGP, the local minimizer is applied to obtain the decomposition point (DP 1). The exit point obtained between the local minima B and C is (0.218, 0.292). It converges to the decomposition point (DP 2) directly when the local minimizer is obtained. Hence, given the three local minima, we are able to find the two saddle points present between them using our method.

B. Test Case 2: Three-dimensional symmetric systems

Three-atom Lennard–Jones clusters: This system is mainly used to demonstrate a simplified version of our algorithm. Our method has some advantages when applied to energy surfaces that are symmetric in nature. To demonstrate this, we used the Lennard–Jones pair potential which is a simple and commonly used model for interaction between atoms. The Lennard–Jones potential is given by the Equation (15). For simplicity, we applied reduced units; i.e., the values of ϵ and r_0 are taken to be unity. A plot of

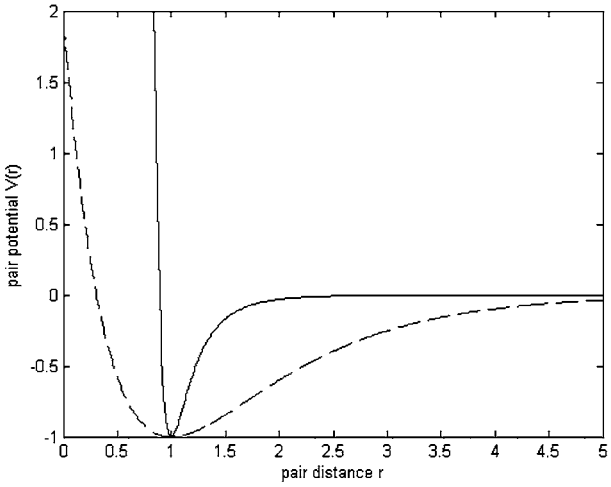

FIG. 9. Characteristic curves of the Lennard–Jones potential and the Morse potential with all parameters set to unity. The solid line represents Lennard–Jones potential (15), and the dashed line represents the Morse potential (17).

the Lennard–Jones Potential of interaction between two atoms generated using Equation (15) is shown in Fig. 9. The original problem is to find the global minimum of the potential energy surface obtained from the interaction between N atoms with two-body central forces. In this example, we consider the potential energy surface corresponding to the three-atom cluster which exhibits symmetric behavior along the x-axis.

$$V = \sum_{i=1}^{N-1} \sum_{j=i+1}^{N} v(r_{ij})$$

$$v(r_{ij}) = \epsilon \left[\left(\frac{r_0}{r_{ij}} \right)^{12} - 2 \left(\frac{r_0}{r_{ij}} \right)^{6} \right] \tag{15}$$

where

$$r_{ij} = \sqrt{(x_i - x_j)^2 + (y_i - y_j)^2 + (z_i - z_j)^2}$$

The total potential energy (V) of the microcluster is the summation of of all two-body interaction terms, $v(r_{ij})$ is the potential energy term corresponding to the interaction of atom i with atom j, r_{ij} is the Euclidean distance between i and j, ϵ describes the strength of the interaction, and r_0 is the distance at which the potential is zero (see Table 2).

For a three atom cluster, let the coordinates be (x_1, y_1, z_1), (x_2, y_2, z_2), and (x_3, y_3, z_3). Though, there are nine variables in this system, due to the translational and rotational variants, the effective dimension is reduced to three. This reduction can be done by setting the other six variables to zero. Hence, the effective variables are (x_2, x_3, y_3).

TABLE 2. STABLE EQUILIBRIUM POINTS AND DECOMPOSITION POINTS FOR THE THREE-ATOM LENNARD–JONES CLUSTER DESCRIBED IN EQUATION (15)

Equilibrium point	*Location*	*Energy value* $c(\cdot)$
SEP A	(1.0, 0.5, 0.866)	−3.000
DP 1	(2.0, 1.0, 0.0)	−2.031
SEP B	(1.0, 0.5, −0.866)	−3.000

We construct the dynamical system corresponding to (15) as follows:

$$\begin{bmatrix} \dot{x_2}(t) \\ \dot{x_3}(t) \\ \dot{y_3}(t) \end{bmatrix} = - \begin{bmatrix} \dfrac{\partial V}{\partial x_2} \\ \dfrac{\partial V}{\partial x_3} \\ \dfrac{\partial V}{\partial y_3} \end{bmatrix} \tag{16}$$

where

$$\frac{\partial V}{\partial x_i} = \sum_{\substack{j=1 \\ j \neq i}}^{3} \frac{12}{(r_{ij})^8} \left[1 - \left(\frac{1}{r_{ij}} \right)^6 \right] . (x_i - x_j)$$

and

$$\frac{\partial V}{\partial y_i} = \sum_{\substack{j=1 \\ j \neq i}}^{3} \frac{12}{(r_{ij})^8} \left[1 - \left(\frac{1}{r_{ij}} \right)^6 \right] . (y_i - y_j).$$

Based on the two given local minima, one can compute the exit point analytically (not numerically) since the system is symmetric. Since the exit point is an exact (not an approximate) value, one can eventually reach the decomposition point by integrating the exit point. The exit point is (0.0,0.0,0.0), (2.0,0.0,0.0), (1.0,0.0,0.0).

In this case, the trajectory-adjustment procedure is not needed. Integrating from the exit point will eventually find the decomposition point. The last two steps of our method, the trajectory-adjustment procedure and the local minimizer, are not required to obtain the decomposition point. It is clear from the example above that in all cases where we compute the exit point numerically, we get an approximation of the exit point which will eventually converge to one of the two local minima after integration. In such cases, the trajectory-adjustment procedure will guide us to maintain the path along the stability boundary and prevent us from being trapped in one of the local minima. Hence, a simplified version of our algorithm is developed for finding saddle points on symmetric surfaces.

C. Test Case 3: Higher dimensional systems

Heptamer island on a crystal: To test our method on a higher dimensional system, we have chosen a heptamer island on the surface of an face-centered cubic (FCC) crystal. This system will not only illustrate the atomic scale mechanism of island diffusion on surfaces but also will help us to understand the kinetics of a process. The atoms interact via a pairwise additive Morse potential described by Equation (17):

$$V(r) = A \left(e^{-2\alpha(r-r_0)} - 2e^{-\alpha(r-r_0)} \right) \tag{17}$$

where $A = 0.71$ eV, $\alpha = 1.61$ Å^{-1}, $r_0 = 2.9$ Å.

These parameters were chosen in such a way that it will reproduce diffusion barriers on real surfaces. The potential was cut and shifted at 9.5 Å. The surface is simulated with a six-layer slab, each layer containing 56 atoms. The minimum energy lattice constant for the FCC solid is 2.74 Å. The bottom three layers in the slab are held fixed. A total of $7 + 168 = 175$ atoms are allowed to move during the search for decomposition points. Hence, this is an example of a 525 (175×3) dimensional search problem. This is the same system used in the review paper by Henkelman *et al.* (2000a). Figure 10 shows the top view of the initial configuration of the island with a compact heptamer sitting on top of the surface. The shading indicates the height of the atoms. The white ones are the heptamer island on the surface of the crystal, and the black ones are at the bottom-most part of the crystal (see Fig. 11).

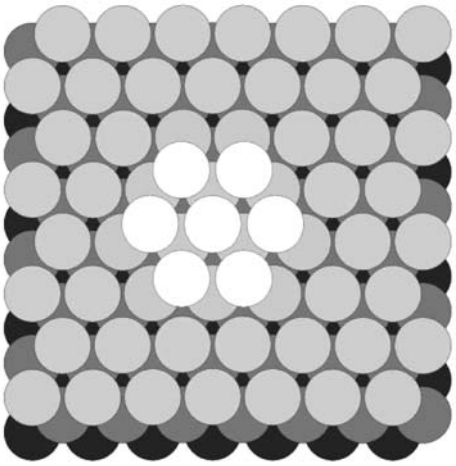

FIG. 10. Top view of the surface and the seven atom island on the surface of an FCC crystal. The shading indicates the height of the atoms.

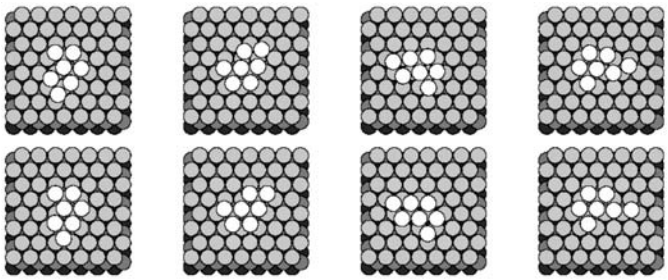

FIG. 11. Some sample configurations of the heptamer island on the surface of the FCC crystal. First row: saddle points configurations. Second row: other local minimum energy configurations corresponding to the above saddle point configurations.

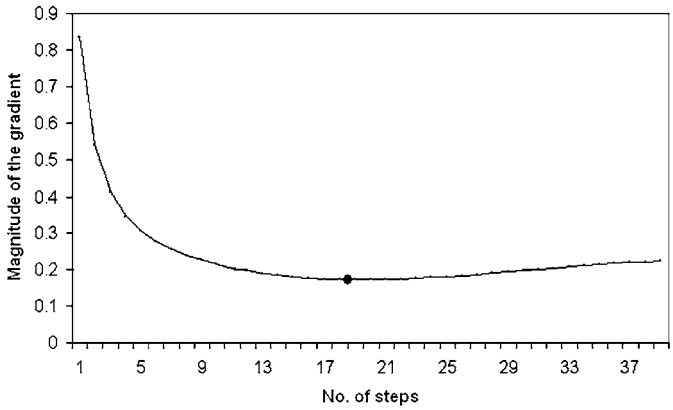

FIG. 12. The gradient curve obtained in one of the higher dimensional test cases.

TABLE 3. RESULTS OF OUR ALGORITHM ON A HEPTAMER ISLAND OVER THE FCC CRYSTAL WITH THE NUMBER OF FORCE EVALUATIONS MADE TO COMPUTE THE MGP GIVEN IN THE LAST COLUMN

Saddle no.	E_{min}	E_{saddle}	E_{MGP}	*RMSD*	Δ*Energy*	Δ*Force*	*No. of evals*
1	−1775.7787	−1775.19	−1775.2139	0.00917	0.02376	0.01833	49
2	−1775.7787	−1775.1716	−1775.1906	0.00802	0.01903	0.01671	43
3	−1775.0079	−1774.8055	−1774.8213	0.0121	0.01578	0.01664	97
4	−1775.006	−1774.8041	−1774.9228	0.03208	0.11868	0.02654	67
5	−1775.0058	−1774.8024	−1774.8149	0.01229	0.01256	0.01704	91
6	−1775.0942	−1774.5956	−1774.3819	0.04285	−0.21362	0.04343	37
7	−1775.0931	−1774.5841	−1774.3916	0.03296	−0.19252	0.03905	43
8	−1775.01	−1774.3106	−1775.0789	0.05287	0.76832	0.04031	97
9	−1775.0097	−1774.3082	−1775.0848	0.05297	0.77662	0.04113	97
10	−1774.3896	−1774.2979	−1774.9551	0.05623	0.65718	0.03103	79
11	−1774.3928	−1774.2997	−1774.9541	0.05615	0.65439	0.03086	79
12	−1774.3933	−1774.2792	−1774.2938	0.02262	0.01450	0.07092	19

Let N be the number of atoms that can move (175) and N' be the total number of atoms (343):

$$V(r) = \sum_{i=1}^{N} \sum_{j=1}^{N'} A\left(e^{-2\alpha(r_{ij}-r_0)} - 2e^{-\alpha(r_{ij}-r_0)}\right) \tag{18}$$

where r_{ij} is the Euclidean distance between i and j. The *dynamical system* is a $3N$ column matrix given by

$$[\dot{x_1}(t)\ \dot{x_2}(t)\ ..\ \dot{x_n}(t)\ \dot{y_1}(t)\ \dot{y_2}(t)\ ..\ \dot{y_n}(t)\ \dot{z_1}(t)\ \dot{z_2}(t)\ ..\ \dot{z_n}(t)]^T$$

$$= -\left[\frac{\partial V}{\partial x_1}\ \frac{\partial V}{\partial x_2}\ ..\ \frac{\partial V}{\partial x_n}\ \frac{\partial V}{\partial y_1}\ \frac{\partial V}{\partial y_2}\ ..\ \frac{\partial V}{\partial y_n}\ \frac{\partial V}{\partial z_1}\ \frac{\partial V}{\partial z_2}\ ..\ \frac{\partial V}{\partial z_n}\right]^T$$

where

$$\frac{\partial V}{\partial x_i} = \sum_{\substack{j=1 \\ j\neq i}}^{n} 2\alpha A\left(e^{-\alpha(r-r_0)} - e^{-2\alpha(r-r_0)}\right).\frac{(x_i - x_j)}{r_{ij}} \tag{19}$$

and derivatives are computed with respect y_i and z_i in a similar manner.

To illustrate the importance of the minimum gradient point and the effectiveness of the boundary tracing, we compared our results with other methods reported by Henkelman *et al.* (2000a). The energy value at the given local minimum is −1775.7911. Value E_{min} is the energy at the new local minimum; E_{saddle} is the energy value at the saddle point. Value E_{MGP} is the energy at the minimum gradient point; *RMSD* is the root mean square distance of all the atoms at the MGP and the saddle point; ΔEnergy is the energy difference between E_{MGP} and E_{saddle}; and Δ Force is the magnitude of the gradient at the MGP. The results of our method are shown in Table 3. The last column indicates the number of gradient computations that were made to reach the minimum gradient point. As seen from the table, our method finds the saddle points with fewer number of gradient computations when compared to other methods. Typically, even the best available method takes at least 200–300 evaluations of the gradient. For detailed results about the performance of other methods, refer to Henkelman *et al.* (2000a). The MGP that was computed in our case varied from 0.01–0.05. The MGP can be treated as a saddle point for most of the practical applications. The RMSD (root mean square distance) value between the MGP and the saddle point is very low. The gradient curve corresponding to this system is shown in Fig. 12.

D. Special cases

Eckhardt surface: The Eckhardt surface (Eckhardt, 1988) is an exceptional case where we need to perturb the exit point in order to follow the stability boundary. Such cases almost never occur in practice,

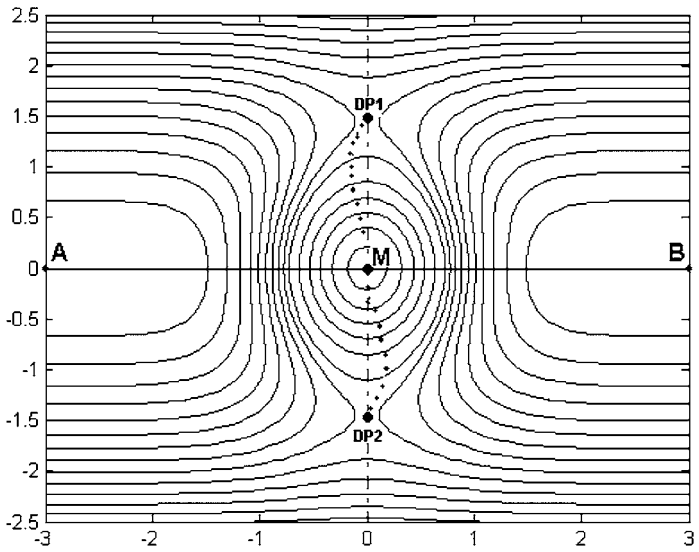

FIG. 13. Two-dimensional contour plot of the potential energy surface of the Eckhardt energy function described by Equation (20). Points *A*, *B*, *M* are stable equilibrium points, and *DP*1, *DP*2 are two decomposition points. The dots correspond to the points on the stability boundary during the trajectory adjustment procedure.

and hence dealing with such surfaces will not be given much importance. Equation (20) gives the Eckhardt energy function. Figure 13 represents the two-dimensional contour plot of the potential energy surface of the Eckhardt function.

$$C(x, y) = e^{-[x^2+(y+1)^2]} + e^{-[x^2+(y-1)^2]} + 4\ e^{-[3(x^2+y^2)/2]} + y^2/2 \tag{20}$$

As shown in Fig. 13, there are two local minima (A,B), and two decomposition points (1,2) on the Eckhardt potential energy surface. A local maximum is present exactly at the center between the two local minima. The two decomposition points are on either side of the maximum. Table 4 shows the energy values at the local minima and the decomposition points.

We construct the dynamical system corresponding to (20) as follows:

$$\begin{bmatrix} \dot{x}(t) \\ \dot{y}(t) \end{bmatrix} = - \begin{bmatrix} \dfrac{\partial C}{\partial x} \\ \dfrac{\partial C}{\partial y} \end{bmatrix} \tag{21}$$

$$\frac{\partial C}{\partial x} = -2x\ e^{-[x^2+(y+1)^2]} - 2x\ e^{-[x^2+(y-1)^2]} - 12x\ e^{-[3(x^2+y^2)/2]}$$

$$\frac{\partial C}{\partial y} = -2(y+1)\ e^{-[x^2+(y+1)^2]} - 2(y-1)\ e^{-[x^2+(y-1)^2]} - 12y\ e^{-[3(x^2+y^2)/2]} + y$$

TABLE 4. STABLE EQUILIBRIUM POINTS AND DECOMPOSITION POINTS FOR THE ECKHARDT SURFACE DESCRIBED IN EQUATION (13)

Equilibrium points	*Location*	*Energy value* $c(\cdot)$
SEP A	(−3.0, 0.0)	0.0
DP 1	(0.0, 1.4644)	2.0409
SEP B	(3.0, 0.0)	0.0
DP 2	(0.0, −1.4644)	2.0409
SEP M	(0.0, 0.0)	4.7358

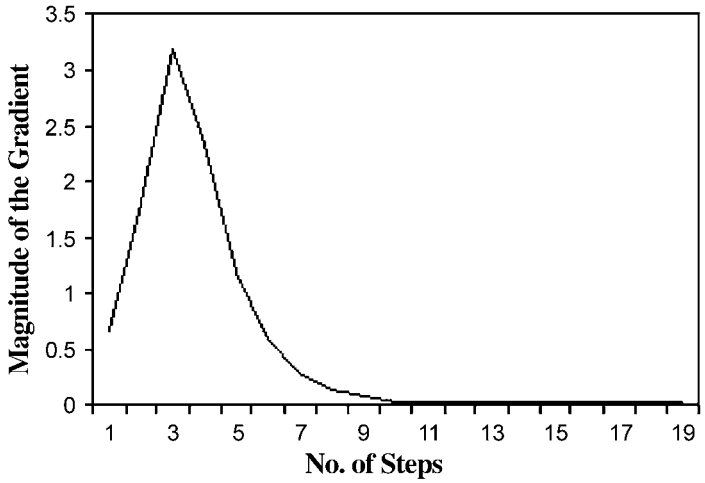

FIG. 14. Gradient curve corresponding to the various points along the stability boundary on the Eckhardt surface.

This surface can be treated as a special case where there are different critical points lying on the vector joining the two local minimum. As seen from the figure, there is a local maximum at (0,0), which is the exit point obtained. It should be noted that this system is also symmetric, and hence one can obtain the exit point analytically. Since the exit point is also a critical point, the exit point is first perturbed and then the trajectory adjustment procedure is used to compute the MGP. The two decomposition points are at (0.0, 1.4644) and (0.0, −1.4644). The gradient curve is shown in Fig. 14.

From this MGP, the local minimizer is applied to obtain the decomposition point (DP1). The other decomposition point (DP2) is similarly obtained. Our method was also successful in finding saddle points on other two dimensional test surfaces like Minyaev Quapp (Minyaev *et al.*, 1997), NFK (Neria–Fischer–Karplus) (Neria *et al.*, 1996), etc.

VII. CONCLUSIONS AND FUTURE RESEARCH

Saddle points play a vital role in realizing the folding pathways of a protein as well as in understanding the transition state structures during chemical reactions. This paper primarily focuses on a new TRUST-TECH based method for finding saddle points on potential energy surfaces using stability boundaries. Our approach is based on some fundamental results of nonlinear dynamical systems. A novel *trajectory adjustment procedure* has been used to move along the stability boundary. Our method was able to find the saddle points on a wide range of surfaces with varying dimensions. The primary advantage of our method comes from the fact that following the stability boundary is computationally more efficient than directly searching for a saddle point from the given local minima. The deterministic nature of the algorithm ensures that the same saddle point is obtained for every run. Very few user-specific parameters makes it easy for a new user to implement. We have also explored the symmetric behaviour of some energy surfaces to obtain the exit point analytically and developed a simplified version of our algorithm to compute the saddle points. The algorithm has also been tested successfully on a heptamer island over the surface of an FCC crystal.

As a continuation of this work, we are planning to implement a hierarchial approach for finding the global minimum on a potential energy surface. Combining our approach with any stochastic algorithm will enable us to search the entire solution space more effectively. This can be done by using the method presented in this paper as a tool for *escaping from a given local minimum to another local minimum in the neighborhood*. Though the current work assumes that the two local minima between which the saddle point is computed are given, it can be easily extended to find saddle points from a single local minimum. We would also like to exploit some other application areas where the energy surfaces are more complicated.

APPENDIX A: LEPS POTENTIAL

The model of LEPS potential simulates a reaction involving three atoms confined to motion along a line. Only one bond can be formed either between atoms A and B or between atoms B and C:

$$C(x, y) = \frac{Q_{AB}}{1+a} + \frac{Q_{BC}}{1+b} + \frac{Q_{AC}}{1+c} - \left[\frac{J_{AB}^2}{(1+a)^2} + \frac{J_{BC}^2}{(1+b)^2} + \frac{J_{AC}^2}{(1+c)^2} + \frac{J_{AB}J_{BC}}{(1+a)(1+b)} + \frac{J_{BC}J_{AC}}{(1+b)(1+c)} + \frac{J_{AB}J_{AC}}{(1+a)(1+c)} \right]^{\frac{1}{2}} \tag{22}$$

where the Q functions represent the Coulomb interactions between electron clouds and the nuclei and the J functions represent the quantum mechanical exchange interactions. The form of the Q and J functions is given below:

$$Q(r) = \frac{d}{2}\left(\frac{3}{2}e^{-2\alpha(r-r_0)} - e^{-\alpha(r-r_0)}\right)$$

$$J(r) = \frac{d}{4}\left(e^{-2\alpha(r-r_0)} - 6e^{-\alpha(r-r_0)}\right)$$

The parameters were chosen to be $a = b = c = 0.05$, $d_{AB} = d_{AC} = d_{BC} = 4.746$, $\alpha = 1.942$, and $r_0 = 0.742$. The details about the LEPS potential are given by Polanyi and Wong (1969).

APPENDIX B: GOLDEN SECTION SEARCH

The following procedure describes the golden section search method. Let a and b be the two intervals between which the *exit point* is located. The golden section search method computes the exit point with an accuracy of $\pm\epsilon$; r is the *golden mean* ($\frac{3-\sqrt{5}}{2}$) (Press *et al.*, 1992); and $f(x)$ returns the function value at point x.

procedure *GoldenSectionSearch*(a, b, ϵ)
1: Initialize $r = 0.38197$ (golden mean)
2: $c = a + r(b - a)$
3: $d = b - r(b - a)$
4: **while** $|b - a| > \epsilon$ **do**
5: **if** $f(c) > f(d)$ **then**
6: $b = d,\ d = c,\ c = a + r(b - a)$
7: **else**
8: $a = c,\ c = d,\ d = b - r(b - a)$
9: **end if**
10: **end while**
11: **return** b

APPENDIX C: PROOFS

Proof of Theorem 3.1

Proof. Let $\Phi(x, t)$ denote the bounded trajectory starting at x. Consider the time derivative $\frac{d}{dt}f(\Phi(x, t))$ along the trajectory. It is clear that $\frac{d}{dt}f(\Phi(x, t)) = -(\nabla f(\Phi(x, t)))^T\ (\nabla f(\Phi(x, t))) \leq 0$ moreover, $\frac{d}{dt}f(\Phi(x, t)) = 0$ if, and only if, $x \in E$. Therefore, $f(x)$ is an energy function of the negative quasi-gradient system (3). ■

Proof of Theorem 3.6

Proof. The first part of the proof is published in Chiang and Chu (1996). Function $f(x)$ is a Lyapunov function (Chiang *et al.*, 1988) for the negative gradient system (3). Hence, every trajectory within the stability region $A(\bar{x})$ converges to $\bar{x}$, and the function value $f(x)$ decreases along every nontrivial trajectory. So, $\bar{x}$ is a stable equilibrium point of (3) if and only if there exists a neighborhood N such that $f(x)$ reaches a local minimum at $x = \bar{x}$. In a similar manner, we can prove that $\bar{x}$ is a source of (3) if and only if $\bar{x}$ is an isolated local maximum for (1) by inverting the dynamical system (to make the stable equilibrium point a source) and the energy function (new energy function for the new dynamical system).

To prove that $\bar{x}$ is a decomposition point of (3) if and only if $\bar{x}$ is a saddle point for (1), one has to consider the properties of the second derivatives. Since, all the critical points of (1) and all the equilibrium points of (3) are the same and Hessian of the original function $f(x)$ and the gradient of (3) at these points are the same, the corresponding eigenvalues and eigenvectors of are equal. This concludes the proof. ■

ACKNOWLEDGMENTS

We would like to thank Dr. Graeme Henkelman of University of Texas at Austin for providing the source code and images of the high dimensional FCC crystal surface. We would also like to thank Dr. Choi, Cornell University, and Dr. Li, Global Optimal Technology Inc., for some useful discussions.

REFERENCES

Baker, J. 1986. An algorithm for the location of transition states. *J. Comp. Chem.* 7(4), 385–395.

Barkema, G., and Mousseau, N. 1996. Identification of relaxation and diffusion mechanisms in amorphous silicon. *Phys. Rev. Lett.* 77, 43–58.

Bokinsky, G., Rueda, D., Misra, V.K., Gordus, A., Rhodes, M.M., Babcock, H.P., Walter, N.G., and Zhuang, X. 2003. Single-molecule transition-state analysis of rna folding. *Proc. Natl. Acad. Sci.* 100, 9302–9307.

Chiang, H., and Chu, C. 1996. A systematic search method for obtaining multiple local optimal solutions of nonlinear programming problems. *IEEE Trans. on Circuits and Systems: I Fundamental Theory and Applications* 43(2), 99–109.

Chiang, H., and Fekih-Ahmed, A. (1996). Quasi-stability regions of nonlinear dynamical systems: Theory. *IEEE Trans. on Circuits and Systems* 43, 627–635.

Chiang, H., Hirsch, M., and Wu, F.F. 1988. Stability regions of nonlinear autonomous dynamical systems. *IEEE Trans. on Automatic Control* 33, 16–27.

Czerminski, R., and Elber, R. 1990. Reaction path study of conformational transitions in flexible systems: Applications to peptides. *J. Chem. Phys.* 92, 5580–5601.

Dewar, M., Healy, E., and Stewart, J. 1984. Location of transition states in reaction mechanisms. *J. Chem. Soc. Faraday Transactions* 80, 227–233.

Dill, K., Phillips, A., and Rosen, J.B. 1997. Protein structure prediction and potential energy landscape analysis using continuous global minimization. *Proc. 1st Ann. Int. Conf. on Computational Molecular Biology*, 109–117.

Doye, J., and Wales, D. 2002. Saddle points and dynamics of Lennard–Jones clusters, solids and supercooled liquids. *J. Chem. Phys.* 116, 3777–3788.

Eckhardt, B. 1988. Irregular scattering. *Physica* D33, 89–98.

Erman, B., Bahar, I., and Jernigan, R.L. 1997. Equilibrium states of rigid bodies with multiple interaction sites. Application to protein helices. *J. Chem. Phys.* 107, 2046–2059.

Fischer, S., and Karplus, M. 1992. Conjugate peak refinement: An algorithm for finding reaction paths and accurate transition states in systems with many degrees of freedom. *Chem. Phys. Lett.* 192, 252–261.

Heidrich, D., Kliesch, W., and Quapp, W. 1991. Properties of chemical interesting potential energy surfaces. *Lecture Notes in Chemistry* 56.

Helgaker, T. 1991. Transition state optimizations by trust-region image minimization. *Chem. Phys. Lett.* 182(5), 503–510.

Henkelman, G., Johannesson, G., and Jonsson, H. 1999. A dimer method for finding saddle points on high dimensional potential surfaces using only first derivatives. *J. Chem. Phys.* 111, 7010–7022.

Henkelman, G., Johannesson, G., and Jonsson, H. 2000a. Methods for finding saddle points and minimum energy paths. *Progress on Theoretical Chemistry and Physics* 111, 269–300.

Henkelman, G., Uberuaga, B., and Jonsson, H. 2000b. A climbing image nudged elastic band method for finding saddle points and minimum energy paths. *J. Chem. Phys.* 113, 9901–9904.

Ionova, I., and Carter, E. 1993. Ridge method for finding saddle points on potential energy surfaces. *J. Chem. Phys.* 98, 6377–6386.

Jonsson, H., Mills, G., and Jacobsen, K.W. 1998. *In* Berne, B.J., Ciccotti, G., and Coker, D.F., eds., *Classical and Quantum Dynamics in Condensed Phase Simulations*, chapter Nudged Elastic Band Method for Finding Minimum Energy Paths of Transitions, World Scientific, New York.

Khait, Y., Panin, A., and Averyanov, A. 1995. Search for stationary points of arbitrary index by augmented Hessian method. *Int. J. Quantum Chem.* 54, 329–336.

Lastras, L. 1998. *Continuation Methods and Saddle Points: A New Framework*. Master's thesis, Cornell University.

Lee, J., and Chiang, H. 2004. A dynamical trajectory-based methodology for systematically computing multiple optimal solutions of general nonlinear programming problems. *IEEE Trans. on Automatic Control* 49(6), 888–899.

Merlo, C., Dill, K.A., and Weikl, T.R. 2005. Phi values in protein folding kinetics have structural and energetic components. *Proc. Natl. Acad. Sci.* 102(29), 10171–10175.

Minyaev, R., Quapp, W., Subramanian, G., Schleyer, P., and Ho, Y. 1997. Internal conrotation and disrotation in H2BCH2BH2 and diborylmethane 1,3 H exchange. *J. Comp. Chem.* 18(14), 1792–1803.

Miron, R., and Fichthorn, K. 2001. The step and slide method for finding saddle points on multidimensional potential surfaces. *J. Chem. Phys.* 115(19), 8742–8747.

Muller, K., and Brown, L.D. 1979. Location of saddle points and minimum energy paths by a constrained simplex optimization procedure. *Theoret. Chem. Acta* 53, 75–93.

Neria, E., Fischer, S., and Karplus, M. 1996. Simulation of activation free energies in molecular systems. *J. Chem. Phys.* 105(5), 1902–1921.

Polanyi, J., and Wong, W. 1969. Location of energy barriers. I. Effect on the dynamics of reactions A + BC. *J. Chem. Phys.* 51(4), 1439–1450.

Press, W., Teukolsky, S., Vetterling, W., and Flannery, B. 1992. *Numerical Recipes in C: The Art of Scientific Computing*, Cambridge University Press, London.

Quapp, W., Hirsch, M., Imig, O., and Heidrich, D. 1998. Searching for saddle points of potential energy surfaces by following a reduced gradient. *J. Comp. Chem.* 19, 1087–1100.

Reddy, C., and Chiang, H. 2005. Finding saddle points using stability boundaries. *Proc. 2005 ACM Symp. on Applied Computing*, 212–213.

Schlick, T. 2002. *Molecular Modeling and Simulation: An Interdisciplinary Guide*, chapter Multivariate Minimization in Computational Chemistry, Springer Verlag, New York.

Address correspondence to:
Chandan K. Reddy
304 Phillips Hall
School of Electrical and Computer Engineering
Cornell University
Ithaca, NY 14850

E-mail: ckr6@cornell.edu